

# Quasi-phase-matched difference-frequency generation in periodically poled Ti:LiNbO<sub>3</sub> channel waveguides

D. Hofmann, G. Schreiber, C. Haase, H. Herrmann, W. Grundkötter, R. Ricken, and W. Sohler

*Angewandte Physik, Universität-GH Paderborn, Warburger Strasse 100, 33098 Paderborn, Germany*

Received February 22, 1999

Mid-infrared radiation near 2.8  $\mu\text{m}$  was generated by difference-frequency generation in an 80-mm-long periodically poled Ti:LiNbO<sub>3</sub> channel waveguide by pump radiation near 1.55  $\mu\text{m}$  (tunable external-cavity laser) and a signal radiation of 3.391  $\mu\text{m}$  (He-Ne laser). We obtained a normalized conversion efficiency of 105%  $\text{W}^{-1}$ , which is to our knowledge the highest value ever reported. © 1999 Optical Society of America

OCIS codes: 130.3730, 190.4390, 130.3060, 190.2620.

Many atmospheric trace gases such as HF, H<sub>2</sub>CO, CH<sub>4</sub>, NO, N<sub>2</sub>O, SO<sub>2</sub>, and CO have their fundamental absorption bands in the mid-infrared (MIR) spectral range.<sup>1</sup> Therefore, sensitive environmental sensing is possible by use of corresponding MIR (coherent) radiation. Existing lasers have various drawbacks such as limited tunability, low spectral resolution, high power consumption, large size, and fragility, and some require (cryogenic) cooling. As a consequence, new compact MIR sources for room-temperature operation are required.

Tunable coherent emission in the MIR can be generated by difference-frequency generation (DFG) in nonlinear bulk crystals or nonlinear waveguides. Unlike with bulk configurations there is no trade-off in waveguides between mode size and interaction length. Hence in long structures the guided-wave conversion efficiency considerably exceeds the efficiency of a bulk-optics approach.<sup>2</sup>

MIR DFG in Ti:LiNbO<sub>3</sub> optical waveguides has been demonstrated with birefringence phase matching; however, the conversion efficiency was rather low ( $\eta \approx 0.2\% \text{W}^{-1}$ ).<sup>3</sup> The main disadvantages of birefringence phase matching can be avoided by use of quasi-phase matching in periodically poled waveguides. This solution was demonstrated with proton-exchanged channel guides in LiNbO<sub>3</sub>, which resulted in conversion efficiencies of 1.3%  $\text{W}^{-1}$  (Ref. 4) and 0.3–8%  $\text{W}^{-1}$ ,<sup>5</sup> depending on the wavelengths involved. In this Letter we report quasi-phase-matched MIR DFG ( $\sim 2800\text{-nm}$  wavelength) in long, periodically poled Ti:LiNbO<sub>3</sub> waveguides with the highest efficiency achieved so far to our knowledge.

Channel waveguides of 15-, 17.5-, 20-, and 22.5- $\mu\text{m}$  width were fabricated upon the ( $-Z$ ) face parallel to the  $X$  axis of an 80-mm-long, 12-mm-wide, 0.5-mm-thick  $Z$ -cut LiNbO<sub>3</sub> substrate by indiffusion of 160-nm-thick Ti stripes (30 h at 1060 °C in an argon atmosphere with a 1-h postdiffusion at 1060 °C in oxygen to reoxidize the material completely). They are single-mode waveguides in the 3- $\mu\text{m}$  wavelength range.<sup>3</sup> Because of outdiffusion of Li<sub>2</sub>O and pyroelectrically induced electric fields during the diffusion process<sup>6</sup> a homogeneous domain inversion layer as much as 50  $\mu\text{m}$  thick was formed upon the ( $+Z$ ) face.

Therefore, waveguide fabrication by Ti indiffusion is usually done on the ( $-Z$ ) face. Unfortunately, this domain-inversion layer prohibits subsequent electric field poling of the double-domain sample at room temperature. As a consequence, it was necessary to remove the inverted layer by mechanical grinding to obtain a single-domain substrate again, which could be poled via electrodes on the ( $+Z$ ) and ( $-Z$ ) faces of the sample with the higher potential on the ( $+Z$ ) face.

Domain inversion always starts on the ( $+Z$ ) face if the applied electric field exceeds the coercive field of LiNbO<sub>3</sub> (i.e.,  $\sim 21 \text{ kV/mm}$ ). It is therefore preferable to have the periodic electrode on the ( $+Z$ ) face [and the homogeneous counterelectrode on the ( $-Z$ ) face] in fabricating a periodically inverted substrate. In this way better-defined domain boundaries with a more homogeneous periodicity are obtained, in particular near the ( $+Z$ ) surface below the periodic electrode. As a consequence the optical waveguides should be on the ( $+Z$ ) face. Taking these considerations into account, before the periodic poling we performed a charge-controlled homogeneous polarization reversal of the whole sample, using liquid electrodes on both surfaces. Thereafter, the waveguide was on the preferred ( $+Z$ ) face.

In a second poling step we made the periodic domain structure by applying a voltage of  $\sim 10\text{-kV}$  controlling current and charge. We used two kinds of electrode material on the  $+Z$  face and found no obvious difference in domain quality: a sputtered and photolithographically structured chromium electrode with an insulating photoresist layer above (Fig. 1a) and a photolithographically structured photoresist with LiCl-filled openings (Fig. 1b). The periods of the electrode mask ranged from 30.6 to 31.6  $\mu\text{m}$ , with a duty cycle of 39% (width of electrode to gap). The whole ( $-Z$ ) face was in electrical contact with a LiCl solution.

Finally, the electrodes were removed and the whole crystal was chemically etched in HF:HNO<sub>3</sub> for a few minutes to reveal the domain structure. By this process, primarily the ( $-Z$ ) faces are attacked. The inset in Fig. 2 shows a micrograph of the waveguide surface with the domain boundaries clearly observable and a nearly optimum duty cycle of 50:50. We also used a nondestructive second-harmonic microscope

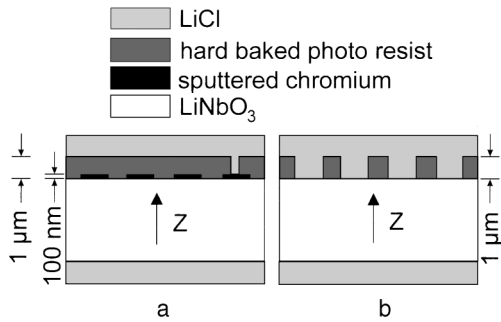


Fig. 1. Electrode structures on Z-cut LiNbO<sub>3</sub>. a, Combination of periodically structured metal and liquid electrodes upon the +Z face; the electrode fingers are interconnected (not shown). b, Periodically structured liquid electrode upon the +Z face.

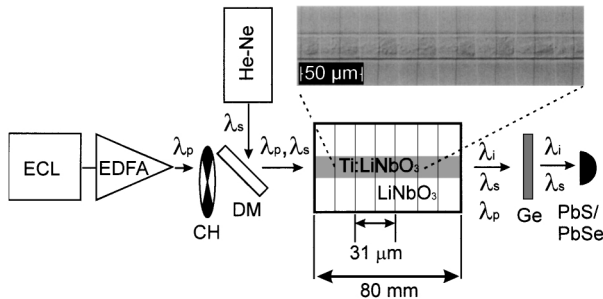


Fig. 2. Experimental setup: ECL, external-cavity laser; EDFA, Er-doped fiber amplifier; He-Ne, He-Ne laser; CH, mechanical beam chopper; DM, dichroic mirror; Ge, germanium filter; PbS/PbSe, lead sulfide or lead selenide photoconductive detector. Inset, surface of a periodically poled and chemically etched Ti:LiNbO<sub>3</sub> waveguide.

to reveal successful domain inversion<sup>7</sup>; in this case chemical etching was not necessary.

Figure 2 shows the experimental setup for DFG experiments. We used a single-frequency fiber-coupled external-cavity semiconductor laser as a pump laser tunable from 1500 to 1580 nm with a maximum output power of 2 mW. The pump radiation was amplified to 11 mW by an Er-doped fiber amplifier in the 1520–1580-nm spectral range. The signal laser was a He-Ne laser with 1-mW output power at  $\lambda = 3391$  nm. We superimposed the two laser beams by using a dichroic beam splitter with high reflection near 3391 nm and high transmission near 1550 nm. The combined beams in TM polarization were focused in the Ti:LiNbO<sub>3</sub> waveguide by an  $f = 8.3$  mm CaF<sub>2</sub> lens. With a second lens of the same type the signal and the generated idler radiations were focused onto a lead sulfide (PbS) or a lead selenide (PbSe) photoconductive detector that was ac coupled to a lock-in amplifier. The pump radiation was absorbed by a Ge filter in front of the detector. As the pump beam was chopped, the idler was periodically generated and the signal was periodically amplified. The two contributions were measured simultaneously by a lock-in technique. However, the spectral responsivity of the PbS detector at the signal wavelength  $\lambda = 3391$  nm is estimated to be only one thirtieth of the responsivity at

the idler wavelength,  $\lambda \approx 2800$  nm, so the detected power corresponds almost exclusively to the idler signal. The spectral responsivities of the PbSe detector at signal and idler wavelengths are nearly the same, so one half of the detected power is due to the generated idler. The responsivity of the PbSe detector was calibrated at  $\lambda = 1550$  nm with a commercial powermeter; it was extrapolated to the MIR wavelength range by the documented spectral response.

The attenuation of the periodically poled waveguides was investigated in TM polarization at  $\lambda = 3391$  nm by the low-finesse resonator method<sup>8</sup>; we measured losses in the range 0.03–0.25 dB cm<sup>-1</sup> with no significant difference between periodically and homogeneously poled waveguides. At this wavelength (signal wavelength of DFG), only the fundamental mode is guided.

The phase-matching curve in Fig. 3 presents the generated idler power (measured with the PbS detector) as a function of the pump wavelength at room temperature for both experiment and theory at a constant signal wavelength ( $\lambda_s = 3391$  nm); the investigated waveguide has a domain period of  $\Lambda = 31.4$   $\mu$ m and losses of 0.03 dB cm<sup>-1</sup>.

The maximum idler power measured with the PbSe detector at optimum phase matching was  $\sim 230$  nW, with an estimated uncertainty of  $\sim 20\%$ . The fine structure of the experimental response results from Fabry-Perot resonances of the waveguide, which represents a low-finesse resonator. These resonances are excited with different efficiencies owing to the mismatch of resonator mode spacings (0.011 nm) and wavelength-tuning steps (0.05 nm) of the pump laser. With coupled power levels of 2 mW for the pump and 110  $\mu$ W for the signal (measured also with the PbSe detector) a maximum conversion efficiency of 105% W<sup>-1</sup> was achieved; this conversion efficiency is normalized to the pump power level. In comparison with literature results in both bulk and waveguide configurations, this is the highest efficiency ever reported to our knowledge; it exceeds published

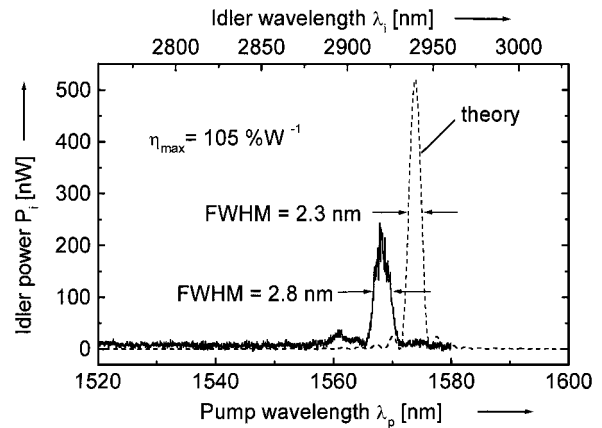


Fig. 3. Idler power versus pump wavelength in a 20- $\mu$ m-wide Ti:LiNbO<sub>3</sub> waveguide with a quasi-phase-matched period of 31.4  $\mu$ m: solid curve, experiment; dashed curve, theory. The theoretical response is calculated with 2-mW pump power, 110- $\mu$ W signal power, an 80-mm interaction length, and attenuations of 0.03 dB cm<sup>-1</sup> for signal and idler and 0.1 dB cm<sup>-1</sup> for pump.

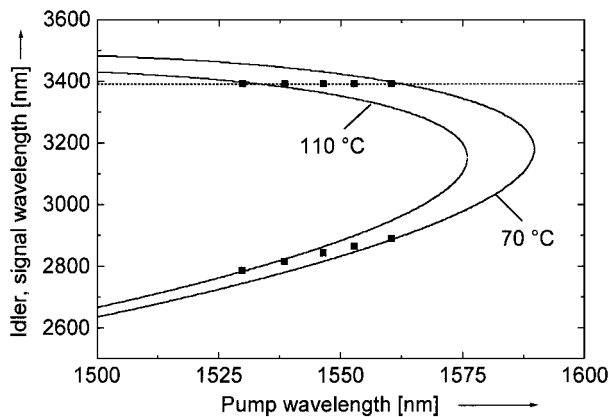


Fig. 4. Calculated tuning curves (solid curves) at fixed temperatures of 70 and 110 °C together with experimental data (70, 80, 90, 100, and 110 °C) at a fixed signal wavelength ( $\lambda_S = 3.391 \mu\text{m}$ ) obtained by DFG in a 30- $\mu\text{m}$  wide, 50-mm-long Ti:LiNbO<sub>3</sub> channel waveguide with a quasi-phase-matched period of 31.2  $\mu\text{m}$ .

efficiencies for DFG in bulk nonlinear crystals (e.g., Ref. 1) by  $\sim 4$  orders of magnitude and for DFG in waveguides (e.g., Refs. 4, 5, 9, and 10) by more than 1 order of magnitude. If our result is normalized to the square of the waveguide length we get an efficiency of  $1.6\% \text{ W}^{-1} \text{ cm}^{-2}$ , somewhat lower than a corresponding result ( $2.3\% \text{ W}^{-1} \text{ cm}^{-2}$ ) achieved with a 7-mm-long periodically poled proton-exchanged waveguide in LiNbO<sub>3</sub> at shorter wavelengths.<sup>10</sup> Theoretical evaluations of the conversion efficiency by use of fundamental mode field distributions only with a Gauss-Hermite-Gauss approximation based on waveguide profiles as described in Ref. 11 provide maximum figures of  $236\% \text{ W}^{-1}$  ( $3.7\% \text{ W}^{-1} \text{ cm}^{-2}$ , respectively) if we assume a loss factor of  $\alpha = 0.03 \text{ dB cm}^{-1}$  for signal and idler waves and of  $\alpha = 0.1 \text{ dB cm}^{-1}$  for the pump. We assume somewhat higher losses for the pump because of higher scattering losses at shorter wavelengths. The half-width of the experimental characteristic of 2.8 nm is best reproduced by a modeled response if an effective interaction length of 68 mm is taken into account. This result demonstrates that 85% of the 80-mm-long periodically poled waveguide contributed to the frequency-conversion process; the waveguide homogeneity is excellent. The small difference between experimental and theoretical phase-match wavelengths can be due to uncertain index data for LiNbO<sub>3</sub> in the MIR spectral range.<sup>12</sup>

Figure 4 shows calculated tuning characteristics for fixed temperatures together with experimental data measured at a fixed signal wavelength with another 30- $\mu\text{m}$ -wide, 50-mm-long waveguide with a

quasi-phase-matched period of 31.2  $\mu\text{m}$ . More than 100-nm tuning of idler wavelength has been achieved by a temperature change of 40 K only. To fit the experimental results best we had to assume a Ti concentration that was 9% larger than in the actual waveguide.

In conclusion, we have generated mid-infrared radiation near 2800 nm by quasi-phase-matched difference-frequency generation of He-Ne laser ( $\lambda = 3391 \text{ nm}$ ) and extended-cavity semiconductor laser ( $\lambda \approx 1550 \text{ nm}$ ) radiation in Ti:LiNbO<sub>3</sub> waveguides with the highest conversion efficiencies of which we are aware. Conversion efficiencies of as much as  $105\% \text{ W}^{-1}$  in 80-mm-long waveguides demonstrate the excellent homogeneity of the periodically poled Ti:LiNbO<sub>3</sub> structures. This result is an important step toward achieving a compact, widely tunable low-threshold, and highly efficient mid-infrared optical parametric oscillator.

This research was supported by the Bundesministerium für Bildung und Forschung under project 13 N 7024. D. Hofmann's e-mail address is d.hofmann@physik.uni-paderborn.de.

## References

1. K. P. Petrov, R. F. Curl, and F. K. Tittel, *Appl. Phys. B* **66**, 531 (1998).
2. W. Sohler, in *New Directions in Guided Wave and Coherent Optics*, D. B. Ostrowsky and E. Spitz, Vol. 79 of NATO Advanced Study Institute Series (Nijhoff, The Hague, 1984), Vol. II, pp. 449-479.
3. H. Herrmann and W. Sohler, *J. Opt. Soc. Am. B* **5**, 278 (1988).
4. D. J. Bamford, K. P. Petrov, A. T. Ryan, T. L. Patterson, L. Huang, and S. J. Field, presented at the 1998 Annual Meeting of the Optical Society of America, October 4-9, Baltimore, Md.
5. M. A. Arbore, M. H. Chou, and M. M. Fejer, in *Conference on Lasers and Electro-Optics*, Vol. 9 of 1996 OSA Technical Digest Series (Optical Society of America, Washington, D.C., 1996), paper JTUE2; in *Annual Report 1995-96* (Center for Nonlinear Optical Materials, Stanford University, Stanford, Calif., 1996), paper A.4.
6. K. Nakamura, H. Ando, and H. Shimizu, *Appl. Phys. Lett.* **50**, 1413 (1987).
7. M. Flörshheimer, R. Paschotta, U. Kubitschek, C. Brillert, D. Hofmann, L. Heuer, G. Schreiber, C. Verbeek, and W. Sohler, *Appl. Phys. B* **67**, 593 (1998).
8. R. Regener and W. Sohler, *Appl. Phys. B* **36**, 143 (1985).
9. K. P. Petrov, A. T. Ryan, T. L. Patterson, L. Huang, S. J. Field, and D. J. Bamford, *Opt. Lett.* **23**, 1052 (1998).
10. E. J. Lim, H. M. Hertz, M. L. Bortz, and M. M. Fejer, *Appl. Phys. Lett.* **59**, 2207 (1991).
11. E. Strake, G. P. Bava, and I. Montrosset, *J. Lightwave Technol.* **6**, 1126 (1988).
12. D. H. Jundt, *Opt. Lett.* **22**, 1553 (1997).